Arabian Journal of Geosciences (2018) 11: 21
https://doi.org/10.1007/s12517-017-3359-4

ORIGINAL PAPER

# The development of attenuation relationship for Northwest Anatolia region

Ayfer Erken[1] · Gülçin Şengül Nomaler[2] · Zeki Gündüz[2]

Received: 24 August 2017 / Accepted: 26 December 2017 / Published online: 11 January 2018


**Abstract**
Ground-motion attenuation relationships using the 1999 Kocaeli earthquake data were developed for the Northwest Anatolia region. This region is seismically active due to its location on Northwest Anatolia Fault Zone and was affected by the 1999 Kocaeli and Düzce earthquakes. Properties of the investigated stations and strong ground-motion data were taken from the Strong Ground Motion Database of Turkey (2017) (TR-NSMN) and Pacific Earthquake Engineering Research Center-Enhancement of Next Generation Attenuation Relationships for Western US (PEER-NGA-West2) database. SeismoSignal software was used in the evaluation of the acceleration records measured in the stations. A generated database for this study contains 369 mainshock and aftershock records, which occurred in the region of 39.39 to 41.03 North (N)/26.04 to 31.73 East (E) coordinates between the years of 1999 (Kocaeli earthquake) and 2006. In this research, peak ground acceleration is greater than 1 gal, and moment magnitude ($M_W$) is greater than 4.0 and Joyner-Boore distance ($R_{JB}$) is 1–344 km. These records were taken from 76 stations located in the investigation area. In addition to these data, 33 mainshock records worldwide were used for recovery of regression coefficients. Therefore, total of 402 data were used in this research. Attenuation relationships obtained from different types of ground were derived from the model generated by Boore et al. (*Seismol Res Lett* 68(1):128–153, 1997) for shallow earthquakes in North America. In this study, attenuation relation equations were developed by applying nonlinear regression analysis, with Statistical Package for the Social Sciences (SPSS) Statistics 20.0 software for B-C and D class soil according to the National Earthquake Hazards Reduction Program (NEHRP) classification system.

**Keywords** Attenuation relationships · Nonlinearity · Peak ground acceleration · Soil · Rock · Liquefaction

## Introduction

Horizontal acceleration is one of the major factors on the damage caused by large earthquakes, which are defined as "strong ground-motion." Seismic waves during earthquakes are affected significantly from the local site conditions while spreading upward. The strong ground-motion parameters can have different values depending on these conditions.

✉ Ayfer Erken
erken@itu.edu.tr

[1] Civil Engineering Faculty, Earthquake Engineering and Disaster Management Institute, Istanbul Technical University, Maslak, Istanbul, Turkey

[2] Department of Civil Engineering, Sakarya University, Sakarya, Turkey

The acceleration records measured in earthquakes, which may be regarded as one of the most important strong ground-motion parameters, contain important engineering information. The estimation of peak ground acceleration should be done by using statistical regression techniques for regions where measurement is not possible due to lack of strong motion stations. In this approach, ground-motion equations were developed by the relationships between evaluating the acceleration values of earthquakes from different sources and different site conditions. Ground-motion equations define peak ground acceleration in terms of size, location-source distance, site conditions, and faulting mechanism. These equations were named in the literature as "ground-motion models" or "attenuation relationships."

The strong ground-motion data was collected over the last two decades; thus, many attenuation relationships were developed. Joyner and Boore (1981) collected western North America strong motion data and developed an attenuation

relationship between distance to acceleration for soil and rock. Fukushima and Tanaka (1990) developed a relationship for Japan considering all types of soil and rock. Lee et al. (1995) obtained attenuation relationship based on peak acceleration, peak velocity, and displacement. They also classified soil as sediment and rock. Gülkan and Kalkan (2002), Kalkan and Gülkan (2004), Özbey et al. (2004), Ulusay et al. (2004), Akkar and Çağnan (2010), and Akkar et al. (2013) developed Turkey-specific attenuation relationship models by using the acceleration records of earthquakes in Turkey. Abrahamson and Silva (1997) developed response spectral attenuation relationship for deep soil, shallow soil, and rock. Sadigh et al. (1997) considered deep soil and rock for their study. Boore et al. (1997), Campbell (1997), and Ambraseys et al. (1996) developed attenuation relationship of site class based on shear-wave velocity. Amiri et al. (2007) developed attenuation relationships for Iran. Next Generation Attenuation Relations started in 2003 and provided a practical application to estimate the ground motion for shallow earthquakes in seismically active areas (Idriss 2008; Boore and Atkinson 2008; Campbell and Bozorgnia 2008). The studies have been updated with the new data (NGA-West2).

During 1999 Kocaeli and 1999 Düzce earthquakes, a large number of buildings in Adapazarı city and some structures located on Marmara Sea and Sapanca Lake shore lines were affected by ground displacement by induced liquefaction and bearing capacity failure of soils. During mainshock and aftershock, ground-motion data from the stations located on the North Anatolian Fault Zone (NAFZ) were obtained to study the effect of liquefaction on attenuation relationship. An addition of 33 main records from large earthquakes (PEER-NGA-West2 database 2017; U.S.Geological Survey earthquake database) was added to 369 NAF (Strong Ground Database of Turkey) data. To develop an attenuation relationship, common equation proposed by Boore et al. (1997) was used and nonlinear site amplification effect was applied from Boore and Atkinson 2008 by applying nonlinear regression analysis with SPSS. In this research, the attenuation relationship was also studied for liquefaction with the 43 strong motion records obtained from liquefied sites in nine large earthquakes in the world.

This study is useful to determine the threshold level of acceleration and $R_{JB}$ distance to initiate liquefaction in loose saturated sand based on magnitude level.

**Table 1** Mainshock records belonging to the earthquakes that were used in this study

| Num. | Epicenter | Date | Time GMT | Lat. degree | Long. degree | Depth km | $M_W$ | Faulting mechanism | Recording number | |
|---|---|---|---|---|---|---|---|---|---|---|
| | | | | | | | | | Soil | Rock |
| 1. | Center, Kocaeli | 17.08.1999 | 00:01 | 40.75 | 29.95 | 17.00 | 7.4 | SS | 15[a]/21[b](21)[c] | 8[a]/11[b](11)[c] |
| 2. | Center, Düzce | 12.11.1999 | 16:57 | 40.80 | 31.18 | 10.40 | 7.1 | SS | 22[a]/12[b](15)[c] | 6[a]/10[b](13)[c] |
| 3. | Savaştepe, Balikesir | 08.09.2000 | 05:46 | 39.39 | 27.66 | 5.00 | 4.7 | SS | 3[a](2)[c] | 1[a](1)[c] |
| 4. | Yığılca, Düzce | 26.08.2001 | 00:41 | 40.95 | 31.54 | 8.80 | 5.2 | SS | 1[a](1)[c] | 2[a](2)[c] |
| 5. | Marmara Sea | 28.02.2002 | 08:37 | 40.80 | 28.14 | 11.50 | 4.5 | Unknown | 0 | 1[a](1)[c] |
| 6. | Marmara Sea | 23.03.2002 | 02:36 | 40.86 | 27.83 | 7.00 | 4.4 | N | 0 | 1[a](1)[c] |
| 7. | Akyazı, Sakarya | 08.03.2003 | 11:18 | 40.68 | 30.60 | 10.00 | 4.1 | Unknown | 2[a](1)[c] | 1[a](1)[c] |
| 8. | M. Kemalpaşa, Bursa | 20.03.2003 | 12:25 | 40.00 | 28.77 | 13.60 | 4.6 | Unknown | 3[a](3)[c] | 2[a](2)[c] |
| 9. | Cumayeri, Düzce | 21.05.2003 | 08:21 | 40.87 | 30.95 | 5.00 | 4.4 | SS | 1[a](1)[c] | 1[a](1)[c] |
| 10. | Bandırma, Balikesir | 09.06.2003 | 17:44 | 40.18 | 28.00 | 9.10 | 4.8 | N | 5[a](5)[c] | 3[a](3)[c] |
| 11. | Saros Gulf | 06.07.2003 | 19:10 | 40.45 | 26.04 | 17.10 | 5.7 | SS/N | 3[a](3)[c] | 3[a](3)[c] |
| 12. | Center, Bolu | 13.04.2004 | 21:47 | 40.81 | 31.62 | 5.00 | 4.4 | SS | 2[a](2)[c] | 0 |
| 13. | Marmara Sea | 16.05.2004 | 03:30 | 40.75 | 29.32 | 11.00 | 4.6 | Unknown | 5[a](5)[c] | 5[a](5)[c] |
| 14. | Harmancık, Bursa | 20.06.2005 | 19:50 | 39.68 | 29.09 | 4.90 | 4.3 | SS | 1[a](1)[c] | 1[a](0)[c] |
| 15. | Center, Sakarya | 08.02.2006 | 04:07 | 40.70 | 30.41 | 6.80 | 4.9 | Unknown | 7[a](5)[c] | 2[a](2)[c] |
| 16. | Bandırma, Balikesir | 20.10.2006 | 18:15 | 40.25 | 27.97 | 16.70 | 5.1 | Unknown | 13[a](11)[c] | 11[a](11)[c] |
| 17. | Gemlik Gulf | 24.10.2006 | 14:00 | 40.42 | 28.99 | 7.90 | 5.2 | N/SS | 18[a](18)[c] | 11[a](10)[c] |
| 18. | Kaynaşlı, Düzce | 21.11.2006 | 09:14 | 40.81 | 31.31 | 8.60 | 4.3 | Unknown | 1[a](1)[c] | 2[a](0)[c] |
| 19. | Karacabey, Bursa | 19.12.2006 | 19:15 | 40.34 | 28.32 | 18.50 | 4.9 | Unknown | 7[a](4)[c] | 8[a](4)[c] |

[a] These values taken from Strong Ground Motion Database of Turkey

[b] These values taken from PEER database ngawest2.berkeley.edu

[c] Recording number in the generation of database


**Fig. 1** Locations of 20 major earthquakes used in this study (Google Earth)

## Strong motion database used in this study

A total of 402 strong motion data was used in this study. The acceleration records of the August 17, 1999 Kocaeli earthquake ($M_W = 7.4$), November 12, 1999 Düzce earthquake ($M_W = 7.1$), and their aftershocks for Northwest Anatolia. Earthquakes in the region until the end of 2006 were taken from the PEER-NGA-West2 database and Strong Ground Motion Database of Turkey (2017). After 2006, there has been no significant earthquake event ($M_W \geq 4.0$) in this researched area.

The coordinates of the recording stations considered in this study for earthquake-affected areas are in the range of 37.81–41.20 N/26.39–34.03 E (Google Earth 2017). Nineteen major earthquakes that have focal depths of 4.90–18.50-km ranges were evaluated in this study (Table 1, Fig. 1). The magnitudes of earthquakes mainly between 4.0 and 5.0 except 6 earthquakes which are greater than 5.0 magnitude. In addition to these data, 33 mainshock records of 7 major earthquakes worldwide with 5.5 to 17.9-km focal depths and high magnitudes were used for the recovery of regression coefficients (Table 2).

Four hundred two units of acceleration records with a magnitude of 4.0–7.6 measured at 110 strong motion stations were used in the regression analysis. Sixty-eight of these strong motion stations were located on the rock (the time average shear velocity $V_{S30} = 362$–$1602$ m/s) and 42 of them on the ground

**Table 2** Mainshock records belonging to the earthquakes from worldwide that were used for B-C soil classes in this study

| Num. | Epicenter[a] | Date[a] | Time[b] UTC | Lat.[a] degree | Long.[a] degree | Depth[a] km | $M_W$[a] | Faulting mechanism[a] | Recording number[a] | |
|---|---|---|---|---|---|---|---|---|---|---|
| | | | | | | | | | Soil | Rock |
| 1. | Landers, USA | 28.06.1992 | 11:58 | 34.20 | − 116.43 | 7.0 | 7.2 | SS | 45 | 33(1)[c] |
| 2. | Kobe, Japan | 17.01.1995 | 20:46 | 34.59 | 135.01 | 17.9 | 6.9 | SS | 16 | 6(1)[c] |
| 3. | Chi-Chi, Taiwan | 20.09.1999 | 17:47 | 23.85 | 120.82 | 8.0 | 7.6 | RO | 162 | 258(11)[c] |
| 4. | Tottori, Japan | 06.10.2000 | 04:30 | 35.27 | 133.35 | 13.0 | 6.6 | SS | 174 | 240(1)[c] |
| 5. | Niigata, Japan | 23.10.2004 | 08:56 | 37.30 | 138.83 | 10.6 | 6.6 | R | 221 | 309(3)[c] |
| 6. | Iwate, Japan | 13.06.2008 | 23:43 | 39.02 | 140.87 | 6.5 | 6.9 | R | 166 | 201(13)[c] |
| 7. | El Mayor-Cucapah, USA | 04.04.2010 | 22:40 | 32.30 | − 115.26 | 5.5 | 7.2 | SS | 155 | 201(3)[c] |

[a] peer.berkeley.edu/ngawest2/databases/ (Updated_NGA_West2_Flatfile_RotD50_d070_public_version.xlsx)

[b] http://earthquake.usgs.gov/earthquakes/search/(USGS 2017)

[c] Recording number in the generation of database

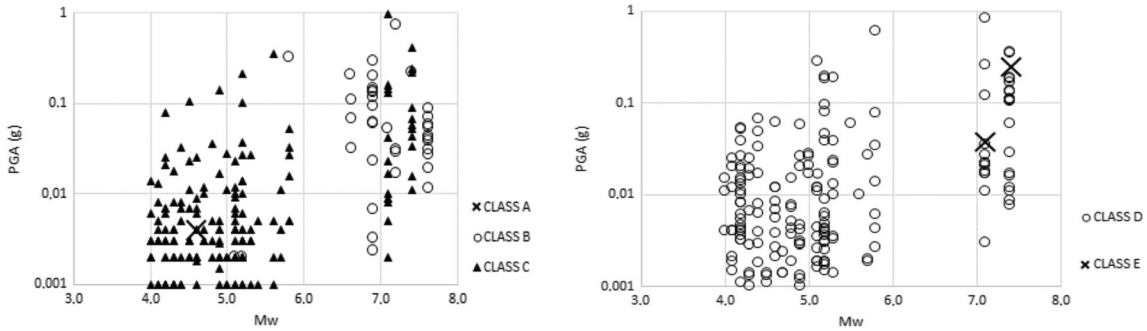


**Fig. 2** Acceleration-magnitude relationship for B-C and D soil classes

($V_{S30}$ = 175–359 m/s). The raw digital data values from Strong Ground Motion Database of Turkey (2017) were passed through 0.1-Hz low-cut and the 25-Hz high-cut frequency range linear Butterworth-Band pass filter window in SeismoSignal software and were used after baseline corrections (SeismoSoft-SeismoSignal 2017). A data catalog was created assuming the threshold value for the largest ground acceleration record is higher than 0.8 gal (peak ground acceleration PGA > 0.8 gal).

The 1999 Kocaeli and Düzce earthquakes had magnitudes of 7.4 and 7.1, respectively. Among the main earthquakes used in this study, which have occurred from the 1999 Kocaeli earthquake until the end of 2006, only the 2003 Gulf of Saros earthquake had a magnitude of 5.7 and the others ranged between 4.1 and 5.2. Among 16 small earthquakes, 6 of them are smaller than a 4.5 magnitude. In conclusion, among 19 earthquakes used in this study, 3 of them are major earthquakes while others are small. All of the used earthquakes worldwide are major. The magnitudes of 181 of total records are between $4.0 < M_W < 5.0$. These recordings were taken for the accuracy of regression analysis.

The time average shear-wave velocity ($V_{S30}$) is a frequently used parameter to represent the ground properties for seismic design and in this study; $V_{S30}$ was used to examine the soil characteristics of the stations. The stations for the acceleration records belong to the 1999 Kocaeli and Duzce earthquakes. The independent earthquakes and aftershocks of the 1999 earthquakes occurred from 1999 until the end of 2006 in the region, and they have been divided into five classes according to the NEHRP (FEMA 450 2004) soil classification system.

A total of 402 records were evaluated. One of them was in group A representing hard rock $V_{S30} > 1500$ m/s, 38 of them were in group B representing rock in the range of $760 < V_{S30} \leq 1500$ m/s, 188 of them were in group C representing very stiff soil or soft rock in the range of $360 < V_{S30} \leq 760$ m/s, 173 of them in group D representing stiff soil in the range of $180 < V_{S30} \leq 360$ m/s, and 2 of them in group E representing soft soil in the range of $V_{S30} < 180$ m/s. Due to a lack of data on soil class A and E, this study represents the B-C and D soil classes.

The relationship between acceleration and magnitude are given in Fig. 2 for the B-C, and D soil classes. Figure 3 presents the relationship between magnitude and distance. The curves were derived from measured acceleration records according to the present magnitude average values. The curves were drawn by obtaining the records at the same $V_{S30}$ and magnitude.

Acceleration records used in this study focused on $R_{JB}$ = 10–200 km, which is defined as the nearest horizontal distance to the surface projection of the fault rupture ($R_{JB}$) and the magnitudes ranged between $M_W = 4.0$–7.6. Because the soil types at the strong motion station are stiff clay, dense soils, and weathered rock, average shear-wave velocities are mostly in the range of 200 m/s < $V_{S30}$ < 700 m/s.

In order to avoid the effects of different soil conditions in the study, $V_{S30}$ value was kept constant. The relationships between $R_{jb}$-PGA depending on the records taken from SKR station, which is located on weathered rock, were obtained for $M_W = 4.0$–5.0–7.0 values (Fig. 4). Sixty-two acceleration records, which were in the content

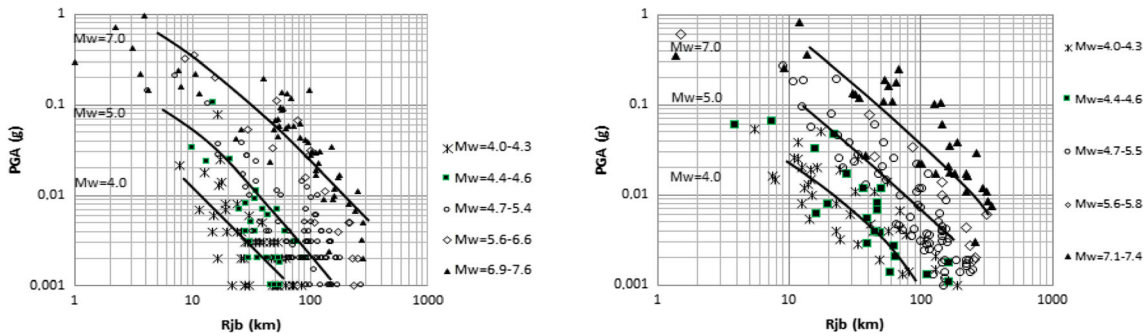


**Fig. 3** Acceleration-distance relationship for B-C and D soil classes

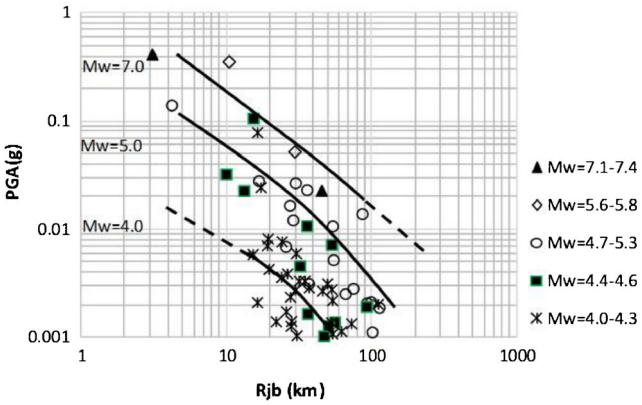


**Fig. 4** Acceleration-distance distribution of recordings taken from Sakarya (SKR) station curves representing earthquake magnitudes (dashed lines represent parts with not enough data)

data catalog and measured at SKR station, were evaluated. The magnitude has more effect than the fault rupture distance at the same soil condition.

## Development of attenuation relationship

In this study, to develop the attenuation relationship, common equation proposed by Boore et al. (1997) were used (Eq. 1).

$$\ln Y = b_1 + b_2(M-6) + b_3(M-6)^2 + b_5 \ln r + b_v \ln \frac{V_S}{V_A} r = \sqrt{R_{jb}^2 + h^2} \quad (1)$$

$Y$ is ground-motion parameter (g), $M$ is moment magnitude, $V_S$ is average shear-wave velocity (m/s), $h$ is fictitious depth which is determined by the regression, $R_{jb}$ is distance (km), and $b_1$, $b_2$, $b_3$, $b_5$, $b_v$, and $V_A$ are coefficients that are determined by the regression. In this equation, $V_A$ is taken as a reference velocity (= 760 m/s corresponding to NEHRP B/C boundary site conditions). $M$, $V_S$, and $R_{jb}$ values are known from dataset, nonlinear part $F_{NL}$ for site amplification added to the equation. According to these approaches that used an equation in this study is presented below.

$$lnPGA = b_1 + b_2(M-6) + b_3(M-6)^2 + b_5 \ln r + b_v \ln \frac{V_{S30}}{V_{ref}} + F_{NL} \quad (2)$$

$F_{NL}$ represents the nonlinear component of site amplification, which depends on $V_{S30}$ and the amplitude of shaking on reference rock (taken as $V_{S30} = 760$ m/s). Nonlinear site amplification effect was applied from Boore and Atkinson 2008-BA08. First, nonlinear slope ($b_{nl}$) computed with $F_{NL}$ was computed with Eqs. 3 to 6 according to shear-wave velocity classes.

$$V_{S30} \le 180 m/s \quad b_{nl} = -0.640 \quad (3)$$

$$180 m/s < V_{S30} \le 300 m/s \quad b_{nl} = (-0.640 - (-0.14)) \frac{\ln\left(\frac{V_{S30}}{300}\right)}{\ln\left(\frac{180}{300}\right)} + (-0.14) \quad (4)$$

$$300 m/s < V_{S30} < 760 m/s \quad b_{nl} = (-0.14) \frac{\ln\left(\frac{V_{S30}}{760}\right)}{\ln\left(\frac{300}{760}\right)} \quad (5)$$

$$760 m/s \le V_{S30} \quad b_{nl} = 0.0 \quad (6)$$

After, $F_{NL}$ was computed with Eqs. 7 to 9, according to *pga4nl* classes. "*pga4nl*" is the predicted PGA in grams for $V_{ref}$ = 760 m/s as given by Eq. 2 with $b_v \ln \frac{V_{S30}}{V_{ref}} + F_{NL} = 0$.

$$pga4nl \le 0.03g \quad F_{NL} = b_{nl} \ln\left(\frac{0.06}{0.1}\right) \quad (7)$$

$$0.03g < pga4nl \le 0.09g \quad F_{NL} = b_{nl} \ln\left(\frac{0.06}{0.1}\right) + c\left[\ln\left(\frac{pga4nl}{0.03}\right)\right]^2 + d\left[\ln\left(\frac{pga4nl}{0.03}\right)\right]^3 \quad (8)$$

$$0.09g < pga4nl \quad F_{NL} = b_{nl} \ln\left(\frac{pga4nl}{0.1}\right) \quad (9)$$

To carefully evaluate the magnitude and distance scaling, only Sakarya (SKR) station records were used in order to avoid the effects of different soil conditions. This station was used due to it being the nearest researched area and is known well for its soil conditions. As shown in Fig. 5, magnitude-dependent distance slope does not occur in the used data set and distance term is not correlated with the magnitude term.

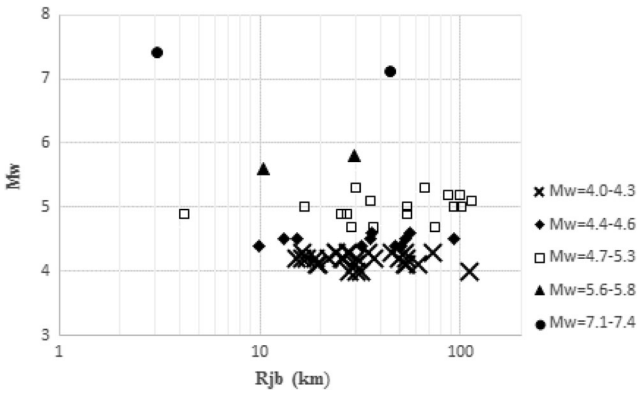


**Fig. 5** Distance and magnitude relationship from SKR station records

**Table 3** Coefficients that calculated from regression analysis

| | $b_1$ | $b_2$ | $b_3$ | $b_5$ | $b_v$ | $h$ | $R^2$ | σ (*lnPGA*) |
|---|---|---|---|---|---|---|---|---|
| B-C soils | 1.835 | 1.034 | − 0.252 | − 1.397 | − 0.069 | 9.718 | 0.807 | 0.730 |
| D soils | 2.135 | 1.008 | − 0.163 | − 1.380 | − 0.133 | 10.510 | 0.826 | 0.630 |

The coefficients in the equation were calculated by means of nonlinear regression analysis. Nonlinear regression analysis on the database was carried out with the software SPSS 20.0. During nonlinear regression analysis with SPSS, parameter estimates and residual sum of squares were used for each iteration. Also, sum of squares for regression, residual, uncorrected total and corrected total, parameter estimates, asymptotic standard errors, and asymptotic correlation matrix of parameter estimates were used for each model. Results are valid only if having specified a function that accurately describes the relationship between dependent and independent variables (IBM SPSS 20 manual-SPSS Statistics for Windows 2017). Since the soft soil recordings are affected by soil conditions, the data were divided into two soil classes. Statistical calculations were made for three classes including the groups B, C, and D.

## Attenuation relationship for B-C and D class soil in NEHRP soil classification system

In the generated catalog by the earthquake data which were taken from the TR-NSMN and PEER-NGA database records, 220 pieces of data consist of B and C soil classes in NEHRP, $M_W = 4.0$ to 7.6 and $R_{JB} = 1$ to 283 km. Main data of the A, B, and C soil classes have $V_{S30} = 370$–1602 m/s (there is only one data in A soil class). Most of the data are related to D group soils that have $M_W$ value between 4.0 and 7.4. Therefore, this study represents the D class with 173 data. Nonlinear regression analysis was performed with the SPSS Statistics 20.0 software by using attenuation Eq. (2) except $F_{NL}$ term. Calculated regression coefficients were given in Table 3. In Table 3, $R^2$ is represented as best fit in SPSS and $\sigma$ (*lnPGA*) is the standard deviation of residual. The final equations for B-C and D soils are presented below, respectively, Eqs. (10) and (11).

$$lnPGA = 1.835 + 1.034(M_W - 6) - 0.252(M_W - 6)^2 - 1.397\ln\sqrt{R_{JB}^2 + 9.718^2} - 0.069\ln\frac{V_{S30}}{760} + F_{NL} \quad (10)$$

$$lnPGA = 2.135 + 1.008(M_W - 6) - 0.163(M_W - 6)^2 - 1.380\ln\sqrt{R_{JB}^2 + 10.510} - 0.133\ln\frac{V_{S30}}{760} + F_{NL} \quad (11)$$

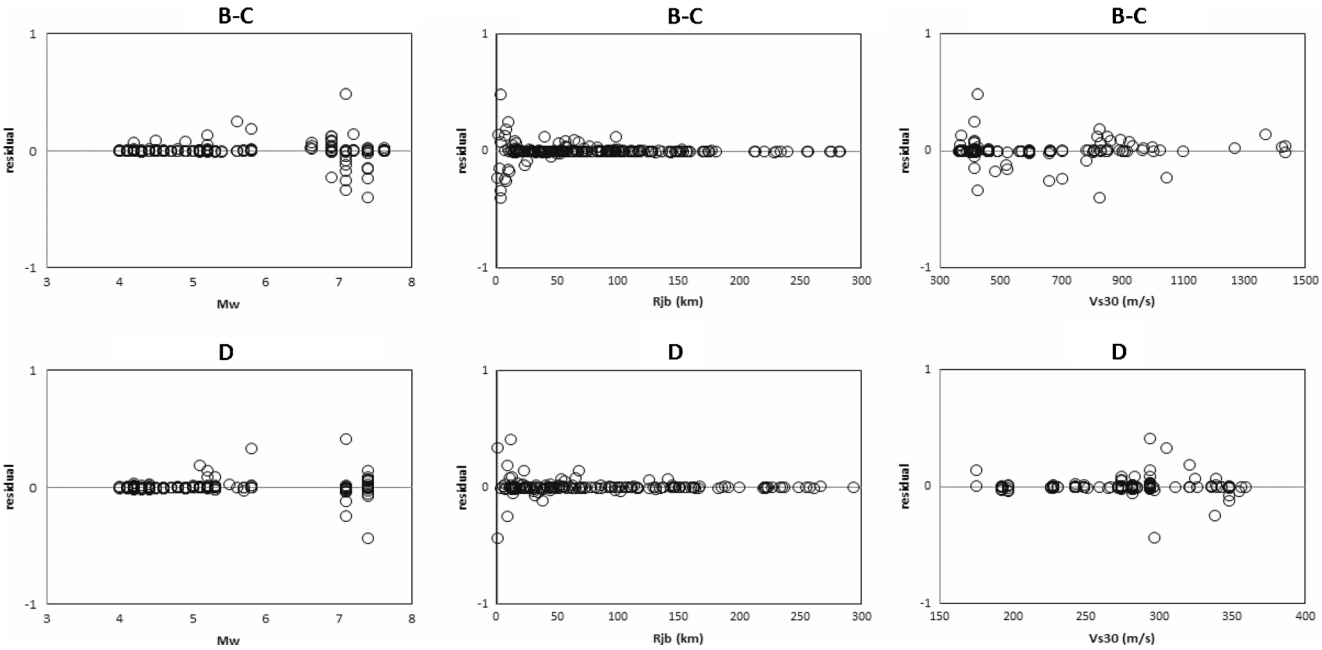


**Fig. 6** Residuals of measured and predicted values of PGA for B-C and D soil classes

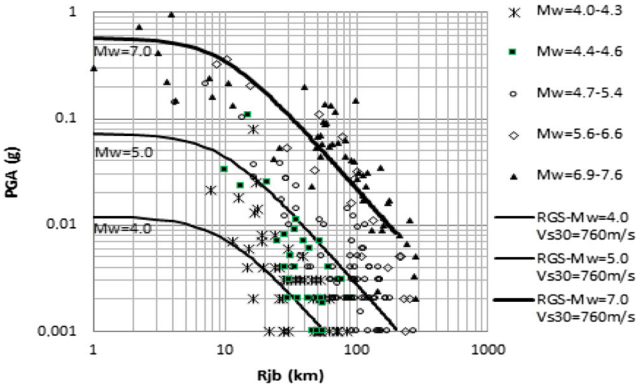


**Fig. 7** Acceleration-distance distribution of recordings and values calculated for $V_{S30} = 760$ m/s and different distances by equation which obtained regression analysis of result belonging to B-C soil classes

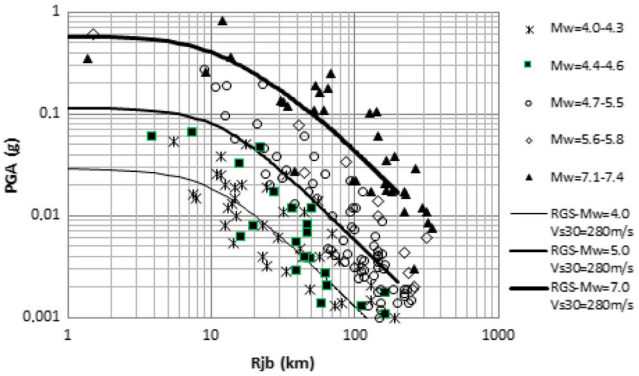


**Fig. 9** Acceleration-distance distribution of recordings and values calculated for $V_{S30} = 280$ m/s and different distances by equation which obtained regression analysis of result belonging to D soil classes

Residuals of measured and predicted values of PGA versus $M_W$, $R_{JB}$, and $V_{S30}$ for each class of soil are shown in Fig. 6, respectively. As shown in Fig. 6, there is no significant bias trends in terms of magnitude, distance, and shear-wave velocity.

Equation 10 was applied at 1–200-km ranges for a magnitude of $M_W = 7.0$–5.0–4.0 and by keeping $V_{S30} = 760$ m/s constant (Fig. 7). It is found in the obtained results that the measurement values and the calculated values are compatible with each other.

This model was also applied to SKR station. Measured and calculated values are almost compatible with each other. They contain small differences due to the effect of the fault length, depth, duration, and the properties of the geological condition between the strong ground station and earthquake epicenter (Fig. 8).

Furthermore, the model which was obtained by nonlinear regression analysis was applied from 1 to 200 km, for magnitude $M_W = 4.0$–5.0–7.0 and by keeping $V_{S30} = 280$ m/s constant (Fig. 9). It is found in the obtained results that the measurement values and the calculated values are compatible with each other as in the case of B and C class soils.

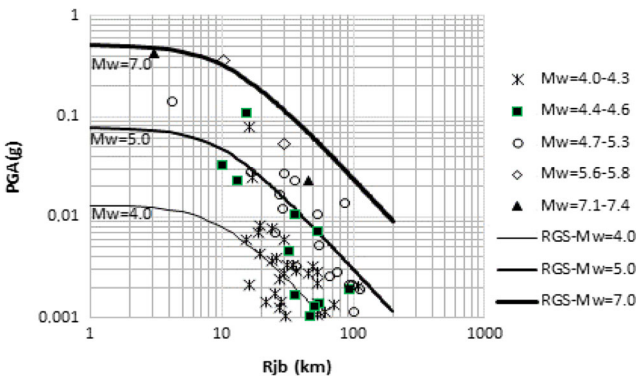


**Fig. 8** Recording values and calculated values by regression analysis for SKR station

## Comparison of other local and global attenuation relationships

The predicted ground motions developed in this study are compared with other attenuation relationships (Table 4, Figs. 10 and 11). The values of peak acceleration that were recorded in the 1999 Kocaeli and 1999 Düzce earthquakes are shown in Figs. 10 and 11, too. These recordings were chosen for different distances and closest shear-wave velocities. The recording stations located on weather rock and soil with shear-wave velocity ranged from 412 to 701 m/s and from 197 to 338 m/s, respectively. Recordings of Northwest Anatolia are the best fit with the presented equation.

Figure 10 shows the relationship between PGA and $R_{JB}$ for $V_{S30} = 760$ m/s and $M_W = 7.0$. This relationship also compared the models developed by Joyner and Boore (1981), Ambraseys et al. (1996, 2005), Sadigh et al. (1997), Akkar et al. (2013), Boore and Atkinson (2008), Kalkan and Gülkan (2004), Özbey et al. (2004), Ulusay et al. (2004), Akkar and Çağnan (2010), Idriss (2008), and Campbell and Bozorgnia (2008). All of these relationships are preferred for $V_{S30} \geq 700$ m/s and $M_W = 7.0$–7.5 (Fig. 10). It can be seen from Fig. 10 that Joyner and Boore (1981), Sadigh et al. (1997), Ambraseys et al. 2005, Özbey et al. (2004), Ulusay et al. (2004), Boore and Atkinson (2008), and Akkar and Çağnan (2010) correlations are not close to the relationship determined to this study.

Figure 11 presents the relationship between PGA and $R_{JB}$ for 280 m/s the shear-wave velocity and $M_W = 7.0$. The relationship was also compared to the results obtained by Ambraseys et al. (1996), Sadigh et al. (1997), Akkar et al. (2013), Kalkan and Gülkan (2004), and Özbey et al. (2004). These relationships are preferred for $V_{S30} = 180$–360 m/s and $M_W = 7.0$. Ambraseys et al. (1996), Akkar et al. (2013), and Özbey et al. (2004) correlations are not close to the relationship determined to this study.

**Table 4** Ground-motion models (PGA) in the literature used in the comparison and their specifications

| Attenuation relationship | Region | $N_{earthquake}$ $N_{recording}$ | $R$ (km) min-max | $M$ min-max | Site |
|---|---|---|---|---|---|
| This study (data used) | Northwestern Turkey and worldwide | 27 402 | $R_{jb}$ 0.1–344.4 | $M_W$ 4.0–7.6 | (B)$V_{S30}$ = 762–1524 m/s<br>(C) $V_{S30}$ = 366–762 m/s<br>(D) $V_{S30}$ = 183–366 m/s<br>(E) $V_{S30}$ < 183 m/s |
| (Boundary cond.) | | | $R_{jb} \leq 200$ | $4.0 \leq M_W \leq 7.0$ | $V_{S30}$ = 183–1524 m/s |
| Joyner and Boore (1981) (data used) | Western North America | 23 182 | $R$ 0.5–370 | $M_W > 5.0$ | Soil<br>rock |
| (Boundary cond.) | | | | $5.0 \leq M \leq 7.7$ | |
| Ambraseys et al. (1996) (data used) | Europe and adjacent regions | 157 422 | $R_{jb}$ 0–260 | $M_S$ 4.0–7.9 | (R) $V_{S30} > 750$ m/s<br>(A) $V_{S30}$ = 360–750 m/s<br>(S) $V_{S30}$ = 180–360 m/s<br>(L) $V_{S30} < 180$ m/s |
| (Boundary cond.) | | | $R_{jb} > 200$ | $4.0 \leq M_S \leq 7.5$ | |
| Sadigh et al. (1997) (data used) | California | 35 523 | $R_{rup}$ 0–200 | $M_W > 3,8$ | (R) rock<br>(DS) deep soil |
| (Boundary cond.) | | | $R_{rup} > 100$ | $4,0 \leq M_W \leq 8,0$ | |
| Akkar et al. (2013) (data used) | Pan-Europan databases | 221 1041 | $R_{jb}$ 0–200 | $M_W$ 4.0–7.6 | $V_{S30} > 800$ m/s<br>360 m/s < $V_{S30} \leq 800$ m/s<br>180 m/s < $V_{S30} \leq 360$ m/s<br>$V_{S30} \leq 180$ m/s |
| (Boundary cond.) | | | Up to at least 200 | $4.0 \leq M_W \leq 8.0$ | $V_{S30}$ = 150–1200 m/s |
| Kalkan and Gülkan (2004) (data used) | Turkish strong motion database | 57 112 | $R_{jb}$ 1.2–250 | $M_W$ 4.0–7.4 | (R) $V_{S30}$ = 700 m/s<br>(S) $V_{S30}$ = 400 m/s<br>(SS) $V_{S30}$ = 200 m/s |
| (Boundary cond.) | | | | | |
| Özbey et al. (2004) (data used) | Northwestern Turkey | 17 195 | $R_{jb} \leq 100$ | $M_W \geq 5.0$ | (A) $V_{S30} > 750$ m/s<br>(B) $V_{S30}$ = 360–750 m/s<br>(C) $V_{S30}$ = 180–360 m/s<br>(D) $V_{S30} < 180$ m/s |
| (Boundary cond.) | | | | | |
| Ulusay et al. (2004) (data used) | Turkish strong motion database | 122 221 | $R_{epi}$ 5.0–100 | $M_W$ 4.1–7.5 | Rock<br>soil—soft soil |
| (Boundary cond.) | | | $R_{epi} \leq 100$ | $4.1 \leq M_W \leq 7.5$ | |
| Akkar and Çağnan (2010) (data used) | Turkish strong motion database | 573 1259 | $R_{jb}$ 0–200 | $M_W$ 3.5–7.6 | (A) $V_{S30} > 750$ m/s (very few)<br>(C) $V_{S30}$ = 360–750 m/s<br>(D) $V_{S30}$ = 180–360 m/s |
| (Boundary cond.) | | | $R_{jb} \leq 200$ | $5.0 \leq M_W \leq 7.6$ | |
| Boore and Atkinson (2008) BA08 (data used) | NGA database and worldwide | 58 1574 | $R_{jb}$ 0–400 | $M_W$ 5.0–8.0 | (A) $V_{S30} > 750$ m/s (very few)<br>(C) $V_{S30}$ = 360–750 m/s<br>(D) $V_{S30}$ = 180–360 m/s |
| (Boundary cond.) | | | $R_{jb} < 200$ | $M_W = 5.0$–8.0 | $V_{S30}$ = 180–1300 m/s |
| Ambraseys et al. (2005) (data used) (Boundary cond.) | Europe and the Middle East | 128 595 | $R_{jb} \leq 100$ | $M_W \geq 5.0$ | (R) $V_{S30} > 750$ m/s<br>(A) $V_{S30}$ = 360–750 m/s<br>(S) $V_{S30}$ = 180–360 m/s<br>(L) $V_{S30} < 180$ m/s |
| Idriss (2008) I08 (data used) | NGA database and worldwide | 72 942 | $R$ 0–200 | $M_W$ 4.5–7.6 | $V_{S30}$ = 450–845 m/s |
| (Boundary cond.) | | | $R$ = 0–200 | $5.0 \leq M_W \leq 8.5$ | $V_{S30}$ = 450–900 m/s |
| Campbell and Bozorgnia (2008) CB08 (data used) | NGA database and worldwide | 64 1561 | $R_{rup}$ 0.1–199 | $M_W$ 4.3–7.9 | (C) $V_{S30}$ = 360–750 m/s<br>(D) $V_{S30}$ = 180–360 m/s |
| (Boundary cond.) | | | $R_{rup}$ = 0–200 | $4.0 \leq M_W \leq 8.5$ | $V_{S30}$ = 150–1500 m/s |

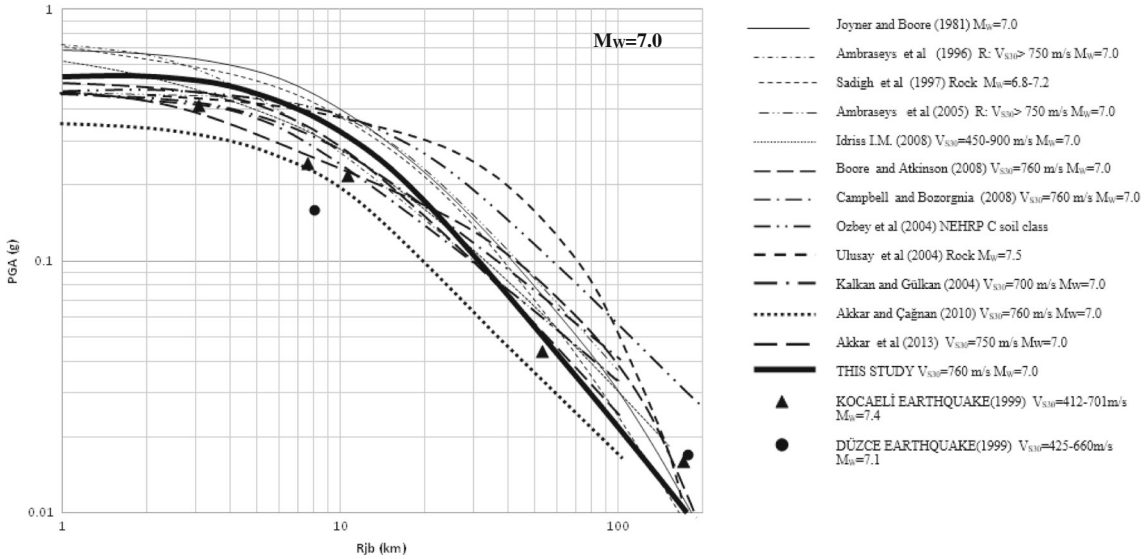


**Fig. 10** Comparison of the PGA values which computed an equation obtained as a result of the regression analysis for $V_{S30} = 760$ m/s and $M_W = 7.0$ with other attenuation relationships and seismic data

Figure 12 presents the relationship, between log (PGA (observed)/PGA (predicted by presented equation)) and $R_{JB}$ with $M_W$ for both B-C and D soil classes. Figure 12 shows that the appropriate range for distance and magnitude.

## The relation between liquefaction and attenuation relationship

The relationship between PGA and $R_{JB}$ is obtained from earthquakes given in Tables 1 and 2, and it is applied for $V_{S30} =$ 200 m/s and $Mw = 6.0–7.0–9.0$. The relationship is compared to PGA data obtained from the 1995 Kobe, Japan; 1999 Chi-Chi, Taiwan; 2004 Niigata, Japan; 2010 Darfield, New Zealand; 2011 Christchurch, and 2011 Tohoku, Japan earthquakes where liquefaction occurred (Table 5) and presented in Fig. 13 (PEER-NGA-West2 database 2017; Engineering database for TSMIP (EGDT 2017); Gelogical hazard information for New Zealand; GeoNet database project (2017), DELTA; New Zealand Geotechnical Database; National Research Institute for Earth Sciences and Disaster Resilience, NIED (2017)). Soil data and measured acceleration values at the strong motion stations were considered in this study.

As shown in Fig. 13, the dashed, solid, and brown lines illustrate $M_W = 6.0–7.0–9.0$ for $V_{S30} = 200$ m/s. The presented model was compared with accelerations obtained from 9 large earthquakes that occurred in Taiwan, Japan, and New Zealand. These earthquakes are mainshocks except December 23, 2011

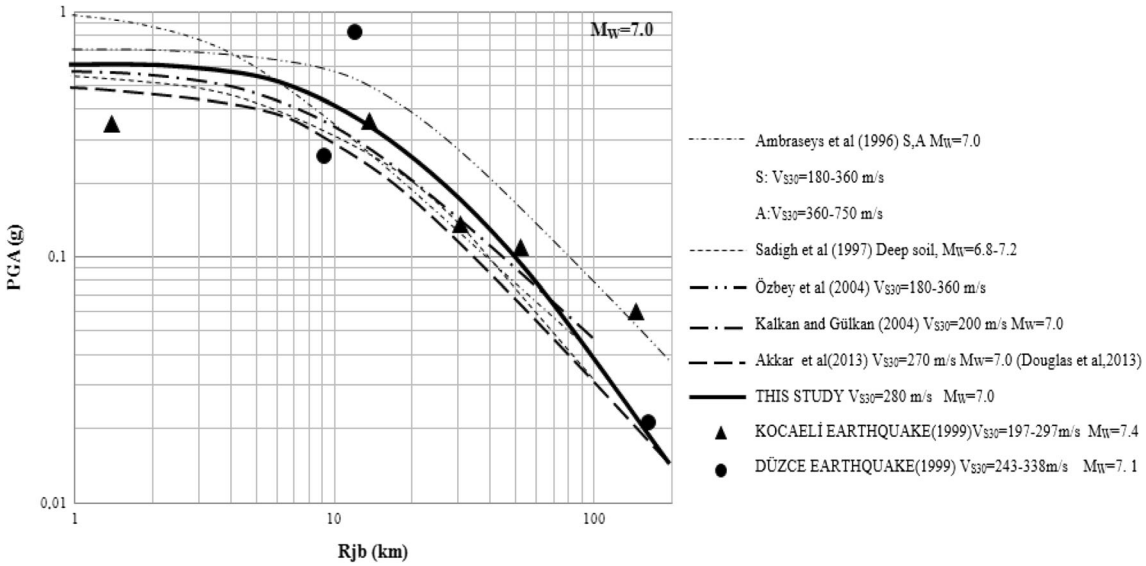


**Fig. 11** Comparison of the PGA values which computed an equation obtained as a result of the regression analysis for $V_{S30} = 280$ m/s and $M_W = 7.0$ with other attenuation relationships and seismic data

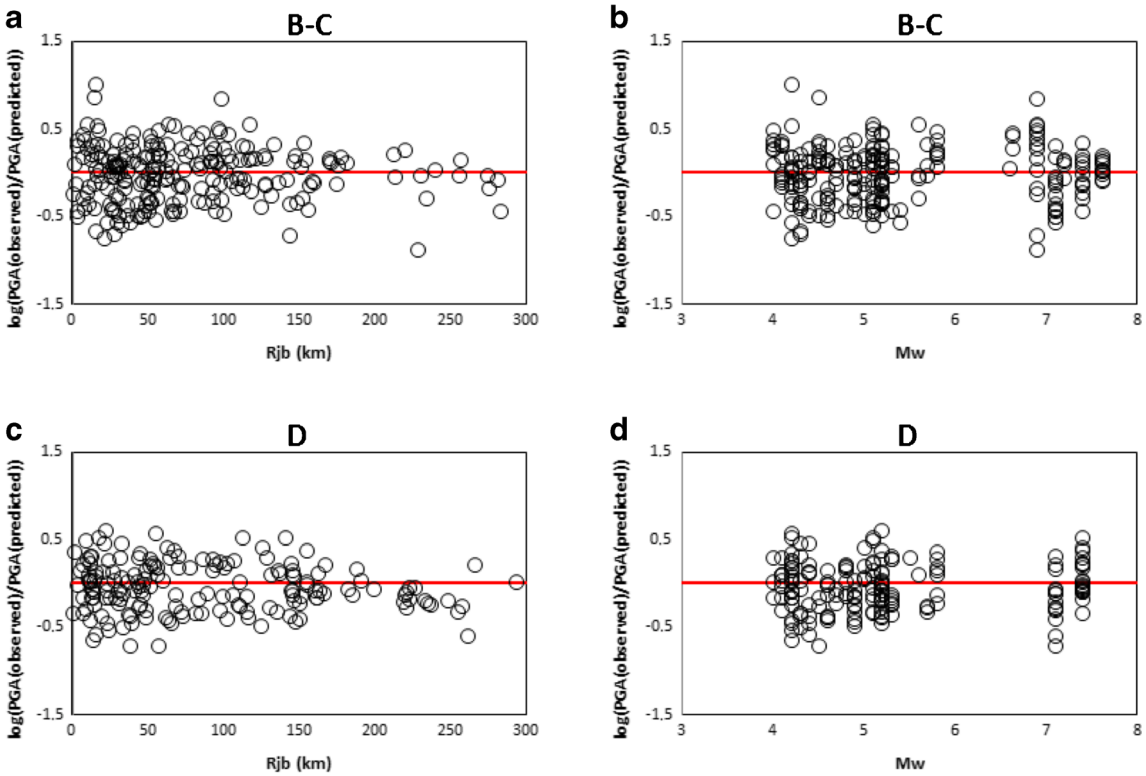


**Fig. 12** Residual scatters of PGA attenuation relationship. **a** PGA residual and distance relation for B-C soil classes. **b** PGA residual and moment magnitude for B-C soils. **c** PGA residual and distance relation for D soil class. **d** PGA residual and moment magnitude for D soils

Christchurch, New Zealand earthquake ($M_W = 5.8$) (Tonkin & Taylor 2012). Fault mechanisms of these earthquakes are generally reverse and magnitudes range between 5.8 and 9.0. The 1995 Kobe and the 2010 Darfield, New Zealand earthquakes have strike slip fault mechanism with the magnitude of $M_W =$ 6.9–7.0.

During earthquakes, liquefaction occurs in some strong motion stations due to the local soil conditions. Liquefaction cannot be observed in some strong motion stations because of the hard soil conditions, but liquefaction was observed around these stations. Shear-wave velocity of soils at strong motion stations varies from 142 to 293 m/s, and moment magnitude changed between 5.8 and 9.0 in 2010 Darfield; 2011 Christchurch, New Zealand; 2011 Tohoku, Japan; and 1995 Kobe Japan earthquakes which PGA values were presented with open markers. During the 1999 Chi-Chi, Taiwan and 2004 Niigata, Japan earthquakes, although liquefaction effects were observed widespread, there were no strong motion stations (Juang et al. 2002; Aydan 2004).

## Soil conditions of the strong motion stations where liquefaction occurred

During New Zealand earthquakes, most of ground deformation and structural damage occurred within the central business district (CBD) of Christchurch. Especially, the 2011 Christchurch earthquake caused severe liquefaction in CBD. The subsurface conditions in the CBD are alternating layers of sands and gravels with silty soils and some peat pockets. The 2010 Darfield and 2011 Canterbury (June, December) earthquakes produced minor to no liquefaction in CBD (Bray et al. 2013). However, the 2010 Darfield earthquake caused widespread liquefaction in the eastern suburbs of Christchurch along the Avon River (Cubrinovski et al. 2011; Bradley and Hughes 2012; Wotherspoon et al. 2013). Soil profile of the examined strong motion stations are given in Fig. 14a. During the 2010 Darfield, 2011 Christchurch, and Canterbury earthquakes, liquefaction did not occur in some areas due to medium dense gravelly and clayey soil conditions as shown and given with dark circle, dark rectangular, and cross markers in Fig. 13.

The 1995 Kobe earthquake occurred in the Osaka area and caused severe liquefaction in Rokko and Port Island (Ishihara et al. 1996; Sato et al. 1996). The shear-wave velocities of the soils under the strong motion stations in Kobe were 256 m/s from different locations except for Port and Rokko Islands. Liquefaction was not observed at the station locations, because they have high $V_{S30}$ values and have clayey-silty-gravelly soils. However, severe liquefaction was observed in Port and Rokko Islands. Their soil profile is given in Fig. 14b (Tokimatsu et al. 1996; Hamada et al. 1996).

The 2011 Tohoku-Oki earthquake ($M_W = 9.0$) generated a large number of soil liquefaction case histories along the

**Table 5** Characteristics of acceleration records from worldwide earthquakes that we used in this study for making comparison D-E and liquefy soils

| Num. | Station name and code | $M_W$ | Fault mechanism | $V_{S30}$ (m/s) and preferred NEHRP | $R_{jb}$ (km) | H (km) | PGA (gal) | |
|---|---|---|---|---|---|---|---|---|
| I-Kobe, Japan 1995-01-17 | | 6.9 | Strike slip | | | 17.90 | | |
| 1 | Port Island[a] | | | 198.00-D | 3.31 | | 309.64 | Liquefy |
| 2 | Rokko Island[b] | | | 198.00-D | 4.00 | | 320.00 | Liquefy |
| II-Chi-chi, Taiwan 1999-09-20 | | 7.6 | Reverse oblique | | | 8.00 | | Nonliquefy |
| III-Niigata, Japan 2004-10-23 | | 6.6 | Reverse | | | 10.60 | | Nonliquefy |
| IV-Darfield, New Zealand 2010-09-04 | | 7.0 | Strike slip | | | 10.90 | | |
| 3 | Hulverstone Drive Pumping HPSC[a,c] | | | 206.00-D | 25.40 | | 138.28 | Liquefy |
| 4 | CPT855 Avondale-PRPC[a,c] | | | 202.08-D | 24.55 | | 186.39 | Liquefy |
| 5 | CPT117 Avonside-PRPC[a,c] | | | 213.67-D | 24.55 | | 192.28 | Liquefy |
| 6 | CPT543 Richmond-SHLC[a,c] | | | 202.95-D | 22.33 | | 192.28 | Liquefy |
| 7 | CPT1086 Dallington Lower-PRPC[a,c] | | | 193.03-D | 24.55 | | 199.14 | Liquefy |
| 8 | CPT846 Wainoni-PRPC[a,c] | | | 199.78-D | 24.55 | | 199.14 | Liquefy |
| 9 | CPT1114 Dallington Upper-SHLC[a,c] | | | 214.44-D | 22.33 | | 178.54 | Liquefy |
| 10 | CPT1293 Kaipoi-KPOC[a,c] | | | 165.17-E | 30.53 | | 210.92 | Liquefy |
| 11 | CPT318 New Brighton-HPSC[a,c] | | | 206.89-D | 25.40 | | 168.73 | Liquefy |
| V-Christchurch, New Zealand 2011-02-22 | | 6.2 | Reverse oblique | | | 5.00 | | |
| 12 | Hulverstone Drive Pump Station HPSC[a,c] | | | 206.00-D | 4.32 | | 246.26 | Liquefy |
| 13 | CPT37 Avondale-HPSC[a,c] | | | 192.95-D | 4.32 | | 364.93 | Liquefy |
| 14 | CPT117 Avonside-PRPC[a,c] | | | 213.67-D | 1.92 | | 430.66 | Liquefy |
| 15 | CPT524 Richmond-SHLC[a,c] | | | 172.50-E | 5.58 | | 414.96 | Liquefy |
| 16 | CPT1086 Dallington Lower-PRPC[a,c] | | | 193.03-D | 1.92 | | 495.41 | Liquefy |
| 17 | CPT849 Wainoni-PRPC[a,c] | | | 187.25-D | 1.92 | | 473.82 | Liquefy |
| 18 | CPT1108 Dallington Upper-SHLC[a,c] | | | 204.32-D | 5.58 | | 426.74 | Liquefy |
| 19 | CPT1344 Kaipoi-KPOC[a,c] | | | 159.09-E | 17.86 | | 185.41 | Liquefy |
| 20 | CPT320 New Brighton-HPSC[a,c] | | | 201.28-D | 4.32 | | 323.73 | Liquefy |
| VI-Christchurch, New Zealand 2011-06-13 | | 6.0 | Reverse | | | 6.00 | | Nonliquefy |
| VII-Christchurch, New Zealand 2011-06-23 | | 5.8 | Reverse | | | 8.00 | | Nonliquefy |
| VIII-Christchurch, New Zealand 2011-06-23 | | 5.9 | Reverse | | | 6.00 | | Nonliquefy |
| IX-Tohoku, Japan 2011-03-11 | | 9.0 | Reverse | | | 24.00 | | |
| 21 | Hazaki[a,d] | | | 100.00-E | 33.27 | | 210,20 | Liquefy |
| 22 | Nakshimo[a,d] | | | 100.00-E | 74.89 | | 446,00 | Liquefy |
| 23 | ST-5[a,d] | | | 100.00-E | 101.00 | | 150.00 | Liquefy |
| 24 | ST-6[a,d] | | | 100.00-E | 102.00 | | 150.00 | Liquefy |
| 25 | ST-7[a,d] | | | 100.00-E | 99.00 | | 220.00 | Liquefy |
| 26 | ST-8[a,d] | | | 100.00-E | 100.00 | | 160.00 | Liquefy |
| 27 | CHB008[a,d] | | | 171.90-E | 112.20 | | 173.64 | Liquefy |
| 28 | CHB009[a,d] | | | 190.10-D | 81.75 | | 187.37 | Liquefy |
| 29 | CHB014[a,d] | | | 194.60-D | 93.67 | | 136.36 | Liquefy |
| 30 | CHB024[a,d] | | | 190.10-D | 95.90 | | 232.50 | Liquefy |
| 31 | IBRH20[a,d] | | | 253.33-D | 31.48 | | 215.82 | Liquefy |
| 32 | KNG002[a,d] | | | 141.90-E | 124.71 | | 165.79 | Liquefy |
| 33 | TKY017[a,d] | | | 190.10-D | 116.85 | | 218.76 | Liquefy |
| 34 | CHI[a,d] | | | 171.90-E | 111.36 | | 154.02 | Liquefy |
| 35 | CHK[a,d] | | | 171.90-E | 113.68 | | 149.11 | Liquefy |
| 36 | IMA[a,d] | | | 171.90-E | 112.54 | | 167.75 | Liquefy |
| 37 | IRF[a,d] | | | 171.90-E | 111.15 | | 251.14 | Liquefy |
| 38 | JAL[a,d] | | | 171.90-E | 110.37 | | 195.22 | Liquefy |
| 39 | MHMX[a,d] | | | 171.90-E | 111.50 | | 172.66 | Liquefy |

**Table 5** (continued)

| Num. | Station name and code | $M_W$ | Fault mechanism | $V_{S30}$ (m/s) and preferred NEHRP | $R_{jb}$ (km) | H (km) | PGA (gal) | |
|---|---|---|---|---|---|---|---|---|
| 40 | MIH[a,d] | | | 171.90-E | 113.96 | | 161.87 | Liquefy |
| 41 | TKK[a,d] | | | 171.90-E | 111.42 | | 208.95 | Liquefy |
| 42 | TKM[a,d] | | | 171.90-E | 111.39 | | 217.78 | Liquefy |
| 43 | TKS[a,d] | | | 171.90-E | 111.97 | | 158.92 | Liquefy |

[a] PEER-NGA-West2 database

[b] Hamada et al. (1996), Sato et al. (1996), Sugito et al. (2000)

[c] Geological hazard information for New Zealand (2017); Khoshnevisan et al. (2015)

[d] National Research Institute for Earth Sciences and Disaster Resilience (NIED)

Pacific Coast in Tohoku and in Kanto including the Tokyo Bay area. The liquefaction was observed at Nakashimo Station near Narusa river with a unit weight that generally ranges between 14 and 17 kN/m$^3$. Dense array strong motion observations have been made at Narashino Station in the reclaimed land and Hazaki Station in Chiba. Shear-wave velocity value was assumed to be 100 m/s for these stations with respect to their soil conditions. Urayasu city, which is located in the Tokyo Bay region, experienced significant and widespread liquefaction damage during the earthquake (Bhattacharya et al. 2011; Cox et al. 2013; Unjoh et al. 2012).

The 1995 Chi-Chi, Taiwan earthquake caused great damage to buildings, bridges, dams, highways, and railways due to liquefaction. The severe liquefaction was observed in Yuanlin, Wufeng, and Nantou (Juang et al. 2002). There are 85 strong motion station data which are shown in Fig. 12 with plus markers in $R_{JB} < 200$ km and PGA < 0.01. Among these stations, TCU110 was located at the Yuanlin Elementary School and its profile is given in Fig. 14c. Although the Yuanlin town experienced widespread liquefaction effects, no evidence of liquefaction was observed at the site of the TCU110 station. Additionally, liquefaction

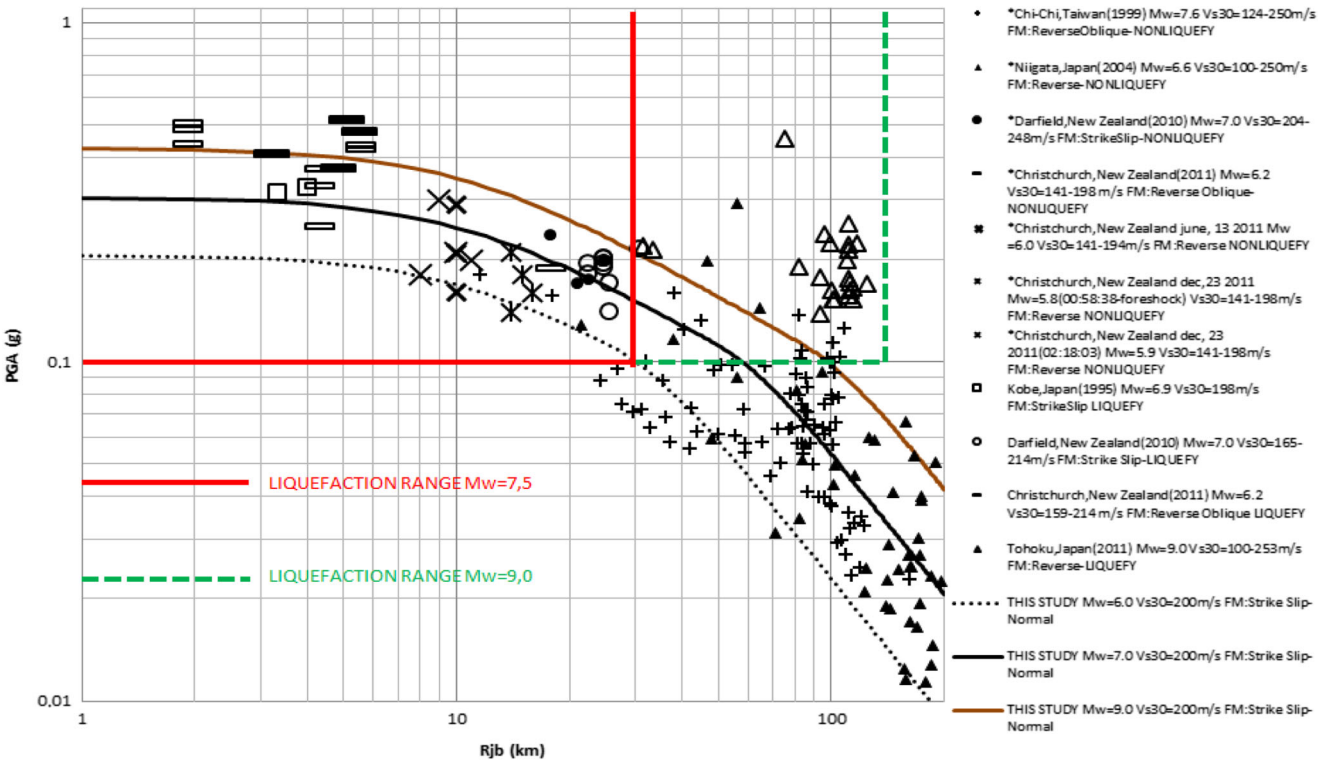


*Liquefaction occured around strong ground motion stations.

**Fig. 13** Comparison of the measured PGA values from strong motion stations with the regression analysis results for $V_{S30} = 200$ m/s and $M_W = 6.0$–7.0–9.0

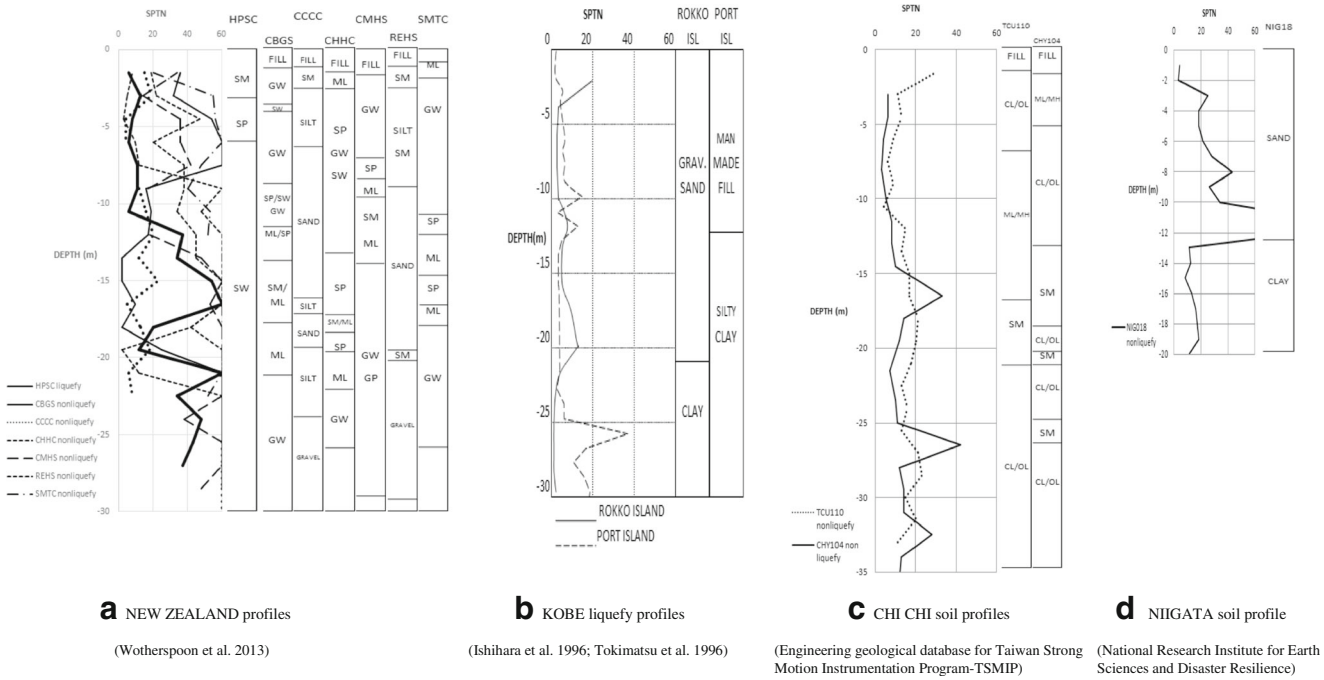


**a** NEW ZEALAND profiles (Wotherspoon et al. 2013)

**b** KOBE liquefy profiles (Ishihara et al. 1996; Tokimatsu et al. 1996)

**c** CHI CHI soil profiles (Engineering geological database for Taiwan Strong Motion Instrumentation Program-TSMIP)

**d** NIIGATA soil profile (National Research Institute for Earth Sciences and Disaster Resilience)

**Fig. 14** Soil profiles of strong motion stations from a)New Zealand, b)Kobe, c)ChiChi, d)Niigata evaluated for liquefaction

occurred at CHY104 which was located in Dounan Town (Fig. 14c).

The 2004 Niigata, Japan earthquake occurred in the Chuetsu region of Niigata Prefecture in Japan (Aydan 2004). During this earthquake, 46 strong motion stations were formed which are shown with dark triangle markers in Fig. 13. Liquefaction was not observed at strong motion stations because of their soil conditions or the far distance and lower peak ground acceleration values. This is also the case for the 1995 Chi-Chi, Taiwan earthquake. Among these stations codes, around NIG018-Kashiwazaki soil profile, liquefaction was observed (Fig. 14d).

As shown in Fig. 13, if the acceleration is greater than PGA > 0.1 g, liquefaction occurs within the 30 km (Joyner-Boore distance) for the $M_W = 7.0$. If the distance is longer than 30 km, sandy soil cannot liquefy even though the magnitude is 7.0. If the moment magnitude increases up to 9.0, liquefaction occurred within 125 km as shown in Fig. 13.

## Conclusion

The model developed in this study was considered to be applicable for estimating peak ground acceleration values for earthquakes in which the following conditions apply:

$5.0 \le M_W \le 7.0$
$0 \le R_{JB} \le 200$ km
B, C, D, E *soil classes* (*NEHRP*)

It was found that equations obtained in this study are compatible with $5.0 \le M_W \le 7.0$ value models in group B, C, and D according to the NEHRP soil classification system. In addition, PGA records measured in large earthquakes at liquefaction sites on D and E soils which have $V_{S30} < 250$ m/s are compatible with the presented model. So, it can be said that the presented model which was developed for D soil class is also valid for E soil class.

Present attenuation relationships verified with earthquakes taken worldwide reveals that acceleration causes liquefaction. If there is a loose saturated sand layer and the shear-wave velocity is less than 200 m/s, when the PGA is greater than 0.1 g within the 30-km distance from the source, liquefaction occurs for the $M_W = 7.0$. The present attenuation is also verified for $M_W = 9.0$ and within the area of PGA ≥ 0.1 g to $R_{JB} =$ 125 km.

## References

Abrahamson NA, Silva WJ (1997) Empirical response spectral attenuation relations for shallow crustal earthquakes. Seismol Res Lett 68(1):94–127. https://doi.org/10.1785/gssrl.68.1.94

Akkar S, Çağnan Z (2010) A local ground-motion model for turkey, and its comparison with other regional and global ground-motion models. Bull Seismol Soc Am 100(6):2978–2995. https://doi.org/10.1785/0120090367

Akkar S, Sandıkkaya MA, Bommer JJ (2013) Empirical ground-motion models for point-and extended-source crustal earthquake scenarios

in Europe and the Middle East. Bull Earthq Eng 12(1):359–387. https://doi.org/10.1007/s10518-013-9461-4

Ambraseys NN, Simpson KA, Bommer JJ (1996) Prediction of horizontal response spectra in Europe. Earthq Eng Struct Dyn 25(4):371–400

Ambraseys NN, Douglas J, Sarma SK, Smit PM (2005) Equations for the estimation of strong ground motions from shallow crustal earthquakes using data from Europe and the Middle East: horizontal peak ground acceleration and spectral acceleration. Bull Earthq Eng 3(1):1–53. https://doi.org/10.1007/s10518-005-0183-0

Amiri GG, Mahdavian A, Dana FM (2007) Attenuation relationships for Iran. J Earthq Eng 11(4):469–492. https://doi.org/10.1080/13632460601034049

Aydan Ö (2004) A reconnaisance report on Niigata-Ken Chuetsu earthquake of October 23, 2004. Tokai University, Department of Marine Civil Engineering, Shizuoka, Japan. http://www.scc.u-tokai.ac.jp/jishin/chuetu/chuetsu_earthquake_report.pdf. Accessed 31 June 2017

Bhattacharya S, Hyodo M, Goda K, Tazoh T, Taylor CA (2011) Liquefaction of soil in the Tokyo Bay area from the 2011 Tohoku (Japan) earthquake. Soil Dyn Earthq Eng 31(11):1618–1628. https://doi.org/10.1016/j.soildyn.2011.06.006

Boore DM, Atkinson GM (2008) Ground-motion prediction equations for the average horizontal component of PGA, PGV and 5%-damped PSA at spectral periods between 0.02 s and 10.0 s. Earthquake Spectra 24(1):99–138. https://doi.org/10.1193/1.2830434

Boore DM, Joyner BW, Fumal TE (1997) Equations for estimating horizontal response spectra and peak acceleration from western North American earthquakes: a summary of recent work. Seismol Res Lett 68(1):128–153. https://doi.org/10.1785/gssrl.68.1.128

Bradley BA, Hughes M (2012) Conditional peak ground accelerations in the Canterbury earthquakes for conventional liquefaction assessment. Technical Report prepared for the Department of Building and Housing, Christchurch, New Zealand. https://www.researchgate.net/publication/272831749_Conditional_Peak_Ground_Accelerations_in_the_Canterbury_Earthquakes_for_Conventional_Liquefaction_Assessment__Part_1_Technical_Report_Prepared_for_the_Ministry_of_Business_Innovation_and_Employment. Accessed 31 June 2017

Bray JD, O'Rourke TD, Cubrinovski M, Zupan JD, Jeon S-S, Taylor M, Toprak S, Hughes M, Ballegooy S, Bouzoiou D (2013) Liquefaction impact on critical infrastructure in Christchurch. Final Technical Report, G12AP20034, U.S.G.S https://www.researchgate.net/publication/277344291_Liquefaction_impact_on_critical_infrastructure_in_Christchurch. Accessed 31 June 2017

Campbell KW (1997) Empirical near-source attenuation relationships for horizontal and vertical components of peak ground acceleration, peak ground velocity and pseudo-bsolute acceleration response spectra. Seismol Res Lett 68(1):154–179. https://doi.org/10.1785/gssrl.68.1.154

Campbell KW, Bozorgnia Y (2008) NGA ground motion model for the geometric mean horizontal component of PGA, PGV, PGD and 5% damped linear elastic response spectra for periods ranging from 0,01 to 10 s. Earthquake Spectra 24(1):139–171. https://doi.org/10.1193/1.2857546

Cox BR, Boulanger RW, Tokimatsu K, Wood CM, Abe A, Ashford S, Donahue J, Ishihara K, Kayen R, Katsumata K, Kishida T, Kokusho T, Mason HB, Moss R, Stewart JP, Tohyama K, Zekkos D (2013) Liquefaction at strong motion stations and in Urayasu City during the 2011 Tohoku-Oki earthquake. Earthquake Spectra 29(S1):S55–S80. https://doi.org/10.1193/1.4000110

Cubrinovski M, Bray JD, Taylor M, Giorgini S, Bradley B, Wotherspoon L, Zupan J (2011) Soil liquefaction effects in the central business district during the February 2011 Christchurch earthquake. Seismol Res Lett 82(6):893–904. https://doi.org/10.1785/gssrl.82.6.893

Engineering geological database for TSMIP (EGDT) (2017) http://egdt.ncree.org.tw/news_eng.htm. Accessed 31 June

FEMA 450 (2004) NEHRP recommended provisions (National Earthquake Hazards Reduction Program) for seismic regulations for new buildings and other structures. Building Seismic Safety Council National Institute of Building Sciences, Washington D.C. http://nehrp.gov/pdf/fema450provisions.pdf. Accessed 31 June 2017

Fukushima Y, Tanaka T (1990) A new attenuation relation for peak horizontal acceleration of strong eathquake ground motion in Japan. Bull Seismol Soc Am 80(4):757–783 http://www.bssaonline.org/content/80/4/757.full.pdf. Accessed 31 June 2017

Geological hazard information for New Zealand (2017) ftp://ftp.geonet.org.nz/strong/processed/Proc. Accessed 31 June

GeoNet database project (2017) DELTA (Data Equipment pLanning Tracking Access). https://magma.geonet.org.nz/delta/app. Accessed 31 June

Google Earth (2017) Google Earth (Online). http://earth.google.com. Accessed 31 June 2017

Gülkan P, Kalkan E (2002) Attenuation modeling of recent earthquakes in Turkey. J Seismol 6(3):397–409. https://doi.org/10.1023/A:1020087426440

Hamada M, Isoyama R, Wakamatsu K (1996) Liquefaction-induced ground displacement and its related damage to lifeline facilities. Soils Found 36(S):81–97. https://www.jstage.jst.go.jp/article/sandf1995/36/Special/36_81/_article. Accessed 31 June 2017. https://doi.org/10.3208/sandf.36.Special_81

Idriss IM (2008) An NGA empirical model for estimating the horizontal spectral values generated by shallow crustal earthquakes. Earthquake Spectra 24(1):217–242. https://doi.org/10.1193/1.2924362

Ishihara K, Yasuda S, Nagase H (1996) Soil characteristics and ground damage. Soils Found 36(S):109–118. https://www.jstage.jst.go.jp/article/sandf1995/36/Special/36_109/_article. Accessed 31 June 2017. https://doi.org/10.3208/sandf.36.Special_109

Joyner WB, Boore DM (1981) Peak horizontal acceleration and velocity from strong-motion records including records from the 1979 Imperial Valley, California, earthquake. Bull Seismol Soc Am 71(6):2011–2038 http://www.bssaonline.org/content/71/6/2011.full.pdf. Accessed 31 June 2017

Juang CH, Tuan H, Lee D-H, Ku C-S (2002) Accessing CPT-based methods for liquefaction evaluation with emphasis on the cases from the Chi-Chi, Taiwan, earthquake. Soil Dyn Earthq Eng 22(3):241–258. https://doi.org/10.1016/S0267-7261(02)00013-1

Kalkan E, Gülkan P (2004) Site-dependent spectra derived from ground motion records in Turkey. Earthquake Spectra 20(4):1111–1138. https://doi.org/10.1193/1.1812555

Khoshnevisan S, Juang H, Zhou Y-G, Gong W (2015) Probabilistic assessment of liquefaction-induced lateral spreads using CPT—focusing on the 2010-2011 Canterbury earthquake sequence. Eng Geol 192:113–128. https://doi.org/10.1016/j.enggeo.2015.04.001

Lee VW, Trifunac MD, Todorovska MI, Novikova EI (1995) Empirical equations describing attenuation of peaks of strong ground motion, in terms of magnitude, distance, path effects and site conditions. Department of Civil Engineering, University of Sothern California, Los Angeles California USA, CE 95-02. https://www.researchgate.net/publication/273710197_Empirical_Equations_Describing_Attenuation_of_the_Peaks_of_Strong_Ground_Motion_in_terms_of_Magnitude_Distance_Path_Effects_and_Site_Conditions. Accessed 31 June 2017

National Research Institute for Earth Sciences and Disaster Resilience (NIED) (2017) http://www.kyoshin.bosai.go.jp. Accessed 31 June

New Zealand Geotechnical Database (2017) https://www.nzgd.org.nz/Registration/Login.aspx?ReturnUrl=%2f. Accessed 31 June

Özbey C, Sarı A, Manuel L, Erdik M, Fahjan Y (2004) An empirical attenuation relationship for northwestern Turkey ground motion

using a random effects approach. Soil Dyn Earthq Eng 24(2):115–125. https://doi.org/10.1016/j.soildyn.2003.10.005

PEER-NGA-West2 database (2017) http://peer.berkeley.edu/ngawest2/databases/. Accessed 31 June

Sadigh K, Chang C-Y, Egan JA, Makdisi F, Youngs RR (1997) Attenuation relationships for shallow crustal earthquakes based on California strong motion data. Seismol Res Lett 68(1):180–189. https://doi.org/10.1785/gssrl.68.1.180

Sato K, Kokusho T, Matsumoto M, Yamada E (1996) Nonlinear seismic response and soil property during strong motion. Soils Found 36(S): 41–52. https://www.jstage.jst.go.jp/article/sandf1995/36/Special/36_41/_article. Accessed 31 June 2017. https://doi.org/10.3208/sandf.36.Special_41

SeismoSoft-SeismoSignal (2017) Earthquake engineering software solutions. http://www.seismosoft.com/downloads. Accessed 31 June 2017. https://doi.org/10.1080/13632469.2016.1158754

SPSS Statistics for Windows (2017) Version 20.0 Chicago:SPSS Inc. https://www.ibm.com/us-en/. Accessed 31 June 2017

Strong Ground Motion Database of Turkey (2017) http://kyhdata.deprem.gov.tr/2K/kyhdata_v4.php. Accessed 31 June 2017

Sugito M, Oka B, Yashima A, Furumoto Y, Yamada K (2000) Time-dependent ground motion amplification characteristics at reclaimed land after the 1995 Hyogoken Nambu earthquake. Eng Geol 56(1–2):137–150. http://www.sciencedirect.com/science/article/pii/S0013795299001398. Accessed 31 June 2017. https://doi.org/10.1016/S0013-7952(99)00139-8

Tokimatsu K, Mizuno H, Kakurai M (1996) Building damage associated with geotechnical problems. Soils Found 36(S):219–234. https://www.jstage.jst.go.jp/article/sandf1995/36/Special/36_219/_article. Accessed 31 June 2017. https://doi.org/10.3208/sandf.36.Special_219

Tonkin & Taylor Ltd (2012) Canterbury earthquakes 2010 and 2011 land report as at 29 February 2012. https://www.canterbury.eqc.govt.nz/sites/public_files/main-report.pdf. Accessed 31 June 2017

U.S. Geological Survey earthquake database (2017) https://earthquake.usgs.gov/earthquakes/search/. Accessed 31 June 2017

Ulusay R, Tuncay E, Sönmez H, Gökçeoğlu C (2004) An attenuation relationship based on Turkish strong motion data and iso-acceleration map of Turkey. Eng Geol 74(3–4):265–291. https://doi.org/10.1016/j.enggeo.2004.04.002

Unjoh S, Kaneko M, Kataoka S, Nagaya K, Matsuoka K (2012) Effect of earthquake ground motions on soil liquefaction. Soils Found 52(5): 830–841. https://doi.org/10.1016/j.sandf.2012.11.006

Wotherspoon L, Orense R, Bradley B, Cox B, Wood C, Green R (2013) Geotechnical characterisation of Christchurch strong motion stations. Earthquake Commission Report, 12/629. https://www.eqc.govt.nz/sites/public_files/3783-Geotech-characterisation-Chch-strong-motion-stations.pdf. Accessed 31 June 2017